International Journal of Current Engineering and Technology
E-ISSN 2277 – 4106, P-ISSN 2347 – 5161

Available at http://inpressco.com/category/ijcet

Review Article

A Review on Tribological Parameters for Fault Diagnosis in Spur Gears

Dharmender Jangra*

Department of Mechanical and Automation Engineering, Northern India Engineering College, New Delhi, India

Received 28 May 2022, Accepted 28 June 2022, Available online 05 July 2022, **Vol.12, No.4 (July/Aug 2022)**

Abstract

The gearbox is a crucial element of many rotating machines and needs to be monitored to eliminate the downtime cost. Due to continuous degradation, the gearbox failed in its desired function. To reduce and prevent the catastrophic failure of machinery, it is important to early detection of the faults. The present work reviews the fault detection techniques based on the tribological parameters.

Keywords: *Tribology, In-situ, Ex-situ, Wear debris*

1. Introduction

The gearbox transmits the power and motion by successive teeth engagement. Gearbox found its application in industrial, civilian and military machinery. Most of the gear pairs are lubricated to reduce friction and wear. Lubrication reduces friction and wears and checks the propagation of mild wear by Selecting a lubricant with suitable properties[1–3]. The lubricant can work in two ways: cool and clean the system[4–23], and maintain the layer of lubrication to avoid contact between interfaces—an optimum amount of lubrication is required to form a suitable layer in elastohydrodynamic lubrication [24]. The periodic monitoring of the lubricant properties works as the diagnostic tool[25–47]for the condition monitoring of the machine element. Different properties of the oil (viscosity, additives, etc.) strongly influence gear failures (pitting, mild-wear, scoring etc.)[1,48,57–66,49,67–74,50–56] The lubricant carries the entire history of the machine elements; it has the reach to the parts which are not directly accessible. The lubricant washed away all wear and foreign particle. The degradation level of lubricant can be related to the deterioration of the active gear profile. Degradation of lubricant affects the film thickness formation; sometimes, the lubricant film breakdown and brings the interface into direct contact, and failures occur [75]. The interface starts deterioration and generates wear debris. The interfaces deteriorate the gears' active profile, and the most common types are fatigue wear (pitting), abrasive wear, and adhesive wear [76–87]. The wear particle associated with each type of wear exhibits different types of shape, size, and morphology[4,88].

The condition monitoring of the system can be carried out in-situ and ex-situ. In in-situ, the lubricant carrying the wear debris passes through an online sensor; the output of the sensor gives information like the temperature of oil[89], the total acid number (TAN)[85,89], total base number (TBN)[85,89], humidity level in oil, the wear particle number count[4,85,89–91], particle per minute[89], total particle mass per hour in micron gram[89], different size particle bin (both ferrous, non-ferrous)[89], and ferrous particle ppm in the lubricant[4,75,85,87,89,90]. In some sense, all this information is utilised to analyse the health of the machine component. In ex-situ analysis the lubricant is analysed under ferrogarm, and Fourier transforms infrared spectroscopy (FTIR). In a ferrogram, the particle size distribution and particle morphology can be analysed. The FTIR output gives the additive depletion and degradation of the oil[4,75,92]. Both in-situ and ex-situ are complementary to each other.

This paper focuses on the direction of reviewing the tribological parameters for the diagnosis of the faults of the gearbox.

2. Gearbox fault through tribological parameters

Gearbox faults are mainly divided into two categories 1. Lubricated (pitting, mild wear etc.) and 2. Non-lubricated (bending, fracture etc.) [93]. The lubricant oil circulating in the system brings complete information about the interacting surfaces. So, the study of changes in the properties of lubricant and different types of wear debris generated on the interface can be used to determine the mechanism of the gear failure. The present study is divided into wear debris-based techniques and lubricant degradation-based techniques.

*Corresponding author's ORCID ID: 0000-0000-0000-0000
DOI: https://doi.org/10.14741/ijcet/v.12.4.2

2.1 Wear debris-based technique of fault detection

The tribological pairs in contact tend to wear out with time. Wear is defined as the progressive loss of material when surfaces in contact have sliding motion at a micro and macro level. The running-in wear improves the contact conditions between the interfaces[93,94]. The transition from normal to severe wear is accompanied by an increase in the size and count of wear particles during operation[95,96]. Figure 1 depicts the wear rate changes over time and at different stages. The count and size of the wear particle[97,98] will give information about two things: loss of lubrication and fatigue failure of the surface. Figure 2 shows the typical gear profile that went under the flank wear, the profile modification in the addendum and the dedendum side of the gear flank. The severity of wear on the addendum and dedendum is high due to the sliding motion between the interface surfaces. The experimental approach to identifying the type of severity of wear depends upon the wear rate, particle per minute, ferrous particle, non-ferrous particle, morphology and texture [4,76,85–91,95,99–108].

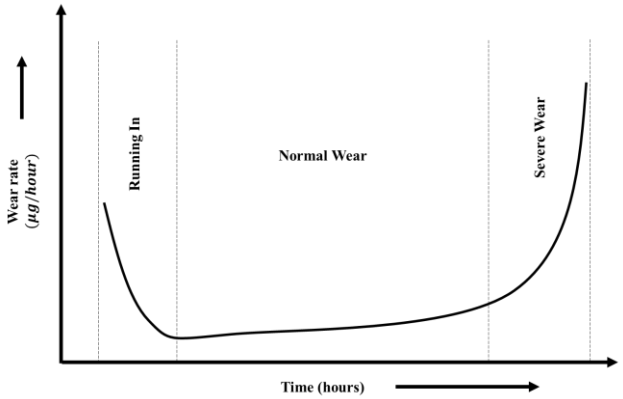

Fig. 1 Bathtub curve: Change of wear rate with operating time[109–111]

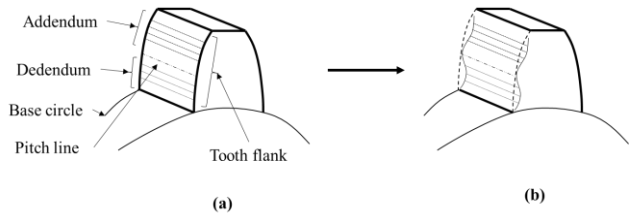

Fig. 2 A typical schematic representation of wear of gear flank

The cyclic loading of the gear teeth takes place during the operation. The Hertzian stress that develops at the contact (line or point contact) is very high. At the pitch point, rolling motion takes place, and above and below the pitch point, the sliding motion takes place[112,113]. Figure 3 depicts the stress, motion, and wear profile at pitch line, addendum, and dedendum.

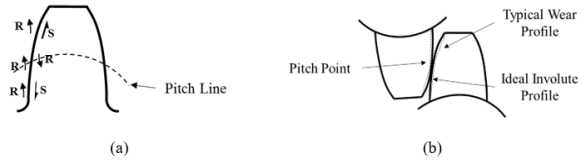

Fig. 3 (a) Gear tooth rolling and sliding contact[93,114], (b) wear profile along the gear flank[115]

Wear particle count is one of the criteria used to find the progression of wear (mild-wear, pitting wear). Large size particles are associated with fatigue failure in the machine. The increase in small-size particles results from the progression of mild-wear along with the micro-pitting. The lubrication degradation and the wear both are complementary to each other. The ferrography (offline and online) is used to determine the faults' severity. In offline ferrography, the samples are taken at regular intervals and processed through the ferrogarph to determine the particle's shape and size and the number of particles in a sample[106,116]. In online ferrography, the ferrograph is attached to the machine, and the lubricant is continuously passed through the ferrograph giving the output like the number of particles, particle size, wear amount (μg/ hour), count of ferrous and non-ferrous particles—the on-line visual ferrography used for the on-line wear debris concentration monitoring. An indicator IPCA is given for the wear debris concentration is the ratio of the area covered by the ferrogram plate by wear debris and the area of the ferrogram plate[111,117].

$$IPCA = \frac{\sum C_i}{W_a \times W_b} \times 100\ \% \qquad (1)$$

The size of the particle in the ferrogram is calculated as the large and small-sized particles, and the percentage of the larger particle size is given as [96]

$$\text{Large particle } (\%) = \frac{D_L - D_S}{D_L + D_S} \times 100 \qquad (2)$$

The worn state is the function of the IPCA; large particle concentration and number of wear particles are given as $f(IPCA, \text{Large particle } (\%), \text{Number of wear particle})$ [96]. The particle count is the better criteria for the early detection of the wear (mild-wear) in the machine component. There is an equilibrium state between the particle count and the lubricant quality (the additive depletion state, TAN, viscosity etc.)[118], every time change in the oil brings a new equilibrium state between the number of particles count and the oil quality. The online ferrography provides the edge over the offline ferrography by providing the real-time state of the system. An offline study for taking the sample from the system needs to wait for periodic maintenance or when the system would shut down due to breakdown. There is some limitation to the online study of the wear the morphological attributes are missing from the output data.

The morphology of the wear particle provides information about the wear mechanism and severity[119]. The magnetic plug[120] is installed in the lubricating system to collect the wear debris. Then the particle is processed and analysed using different techniques (SEM, EDX etc.) to know the composition, size and shape. Figure 4 and Figure 5 show the relationship between wear mode and wear mechanism and wear particle and the shape of the wear particle, the possible machine state. In Figure 6, many statistical parameters are defined for the morphology of the wear particle.

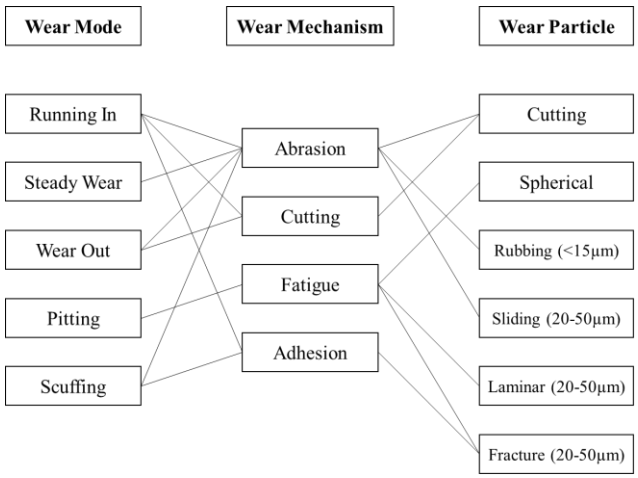

Fig. 4 Relationship between different particle sizes, morphology and mechanism[97,106,116,121–126]

2.2 The lubrication-based fault diagnosis technique

Lubricating oil serves two primary functions in the system: minimising friction between the interfaces and reducing the wear by interposing a lubricant layer on the interface. Lubricant serves many things in the system besides reducing friction and wear, taking away heat, dirt and wear debris. Gear teeth have unique rolling and sliding motion combinations during the contact cycle, due to which the gear operates under elastohydrodynamic and mixed lubrication regimes[127]. The factor affecting the performance of the lubricant in such contact is viscosity (dynamic viscosity and kinematic viscosity)[128], lubricant additives (viscosity index (VI) improver, defoaming, oxidation inhibitors, dispersant, extreme pressure), flash point, total acid number (TAN), total base number (TBN)[108,129].

The wear rate of the component is dependent upon the lubrication mechanisms. The thickness of the lubricant film[130–132] affects the performance and service life of the machine component. The film thickness is defined as[133–135]

$$h_{min} = \frac{1.6\xi^{0.6}(\eta_0 u)^{0.7}(E')^{0.03}R^{0.43}}{w^{0.13}} \quad (3)$$

This film thickness helps in calculating the film parameter called specific film parameter, defined as

$$\Lambda = \frac{h_{min}}{\left(R_{q,1}^2 + R_{q,2}^2\right)^{1/2}} \quad (4)$$

The specific film parameter helps in distinguishing the lubrication mechanism[136]

$5 < \Lambda < 100$ hydrodynamic lubrication
$3 < \Lambda < 10$ elastohydrodynamic lubrication
$\Lambda < 1$ boundary lubrication

The lubricant works as a sacrificial component in the system, degrading gradually with degradation: the lubricant loses its primary function and acts as a catalyst for further degradation of the component. Lubricant oxidation, thermal breakdown, micro-dieseling, additive depletion, and contamination are a few causes of lubricant degradation. Oxidation is the reaction of oil molecules with oxygen molecules. It can lead to an increase in viscosity and the formation of varnish, sludge and sediment. Due to oxidation, the wear rate also increases. Micro-dieseling is when an air bubble transitions from a low-pressure region in a system to a high-pressure zone. Micro dieseling results in adiabatic compression of the air bubble within the oil, which then cooks the surrounding oil molecules, causing instant oxidation. The additive is meant to be sacrificial purposes. The additive used as the antifriction, anti-wear, and extreme pressure additives will deplete over time, and these can cause the loss in performance of the lubricant oil and support the wear of the components. Contamination such as dirt, water, air etc., can significantly influence the rate of lubrication degradation. Dirt containing fine metal particles can be a catalyst that sparks and speeds up the degradation process of the lubricant. Air and water can provide a source of oxygen that can react with the oil and leads to oxidation of the lubricant.

The lubricant degradation over time changes the oil's chemical composition. Fourier transform infrared spectroscopy (FTIR) is used to analyse the oil degradation and the presence of a new bond in the oil. FTIR provides information about new chemical bonds and functional groups in the investigated sample. The covalent bonds absorb infrared radiation at the characteristic wavelength, depending on the molecule's chemical composition and the chemical bond's strength [92,108,134].

Particle Geometry Type	**Particle Feature**	**Wear Type**	**Wear Level**	**Possible Machine Condition**	
Regular	Thin, plan and oblique shape size <50μm	Rubbing, mild adhesion	Normal	Normal wear particle without dramatic increase	
Irregular	Irregular edge with scratches, laminar or chunk shape size> 50μm	Adhesion and fatigue fracture	Severe	Abnormal condition	
Elongated	Slender or curved particle Size <50μm	Plowing	Severe	Impending trouble of severe cutting wear	
Spherical	Ball like, hollow spheres	Rolling fatigue	Abnormal	Indicate the early surface pitting	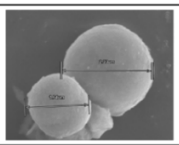

Fig. 5 Correlation of geometrical classification of wear particle shapes to wear mode [89,97,100,114,120–122,122,124,125,137–140]

Method	**Attribute**	**Descriptor**	**Abbreviation**	**Definition**
Form Factor	Profile	Aspect Ratio	AR	Length / Breadth
		Roundness Factor	RF	$(\text{Perimeter})^2/4\pi(\text{Area})$
Fourier Analysis	Profile and Edge Detail	1st, 2nd ,…, Harmonics	$C_1, C_2,\ldots, C_8$	$C_n = \sqrt{(C\, x_n^2 + C_n^2)}$
			$\mu_0, \mu_1, \mu_2, \mu_3$	$R_0 = a_0^2 + \frac{1}{2}\sum_{n=1}^{x}(a_n^2 + b_n^2)$ $\mu_0 = L_0 R_0$, $\mu_1 = 0,\ \mu_2 = R_0^2 \sum_{n=1}^{x} L_{2,n}$ $\mu_3 = R_0^3 \sum_{n=1}^{x}\sum_{m=1}^{x} L_{3,m,n}$
Curvature Analysis	Edge Detail	Standard Deviation	R_q	$R_q = \sqrt{\sum_{i=1}^{n}(x_i - \bar{x})^2/n-1}$
		Skewness	R_{sk}	$R_{sk} = \sum_{i=1}^{n}(x_i - \bar{x})^3/nR_q^3$
		Kurtosis	R_{ku}	$R_{ku} = \sum_{i=1}^{n}(x_i - \bar{x})^4/nR_q^4$
Fractal Analysis	Edge Detail and Profile	Structure	δ_s	$\delta_s = 1 + \lvert m_s \rvert$:m_s:m_s is slope of the line of best fit from the plot of log normalized perimeter vs. log step length (large step length)
		Texture	δ_T	$\delta_T = 1 + \lvert m_T \rvert$:m_T is slop of the line of best fit from the plot of log normalized perimeter vs. log step length (very small step length)
Size Analysis	Size	Weibull Parameter	α	$P(\chi)P(\chi) = 1 - exp\left\{-\left(\frac{\chi - \chi'}{\alpha}\right)^{\beta}\right\}$
			β	

Fig. 6 Shape classification parameters [99,100,105,120,122,139,141–146]

After the sample collection, the lubricant can be passed through the different tests and analysed in such a way that the condition of both lubricant and the machine can be determined.

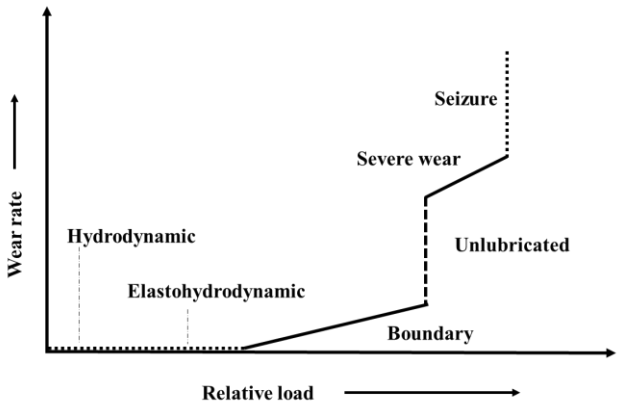

Fig. 7 Wear rate under different lubrication conditions

The samples of lubricant are taken in the turbulent state of the lubricant form by a vacuum pump or suitable tap-off; if not possible in the running condition, the lubricant sample is taken after the temperature of the sump reaches the operating temperature of the system.

The turn-round time should not be more than 48 hours for all tests. For gearbox condition monitoring, the following parameters need to be determined viscosity, water contents (humidity), TAN, TBN, ferrous particle count (Fe ppm), presence of chemical bonds etc.

The kinematic viscosity of a fluid is the quotient of its dynamic viscosity divided by its density. High specific viscosity is required to reduce components' excessive wear and friction. The viscosity of the lubricating oil is affected by the contamination by foreign particles and oil, oxidation, and solvents. The viscosity index (VI) is calculated to find the relationship between the viscosity and lubricant temperature. The viscosity is detrimental for wear and high-temperature operation of lubricant life. It is also essential to know the water content in the lubricant. The presence of water can accelerate wear and corrosion. The water is ingress from seals, gaskets or by condensation. The presence of water in the lube is determined by the sample's relative humidity (RH%). TAN is typically indicating high-temperature use or oxidation of the lubricant. High oxidation leads to a rise in the viscosity of the lubricant. Lubricant oxidation is characterised by discolouration of lubricant and release of brunt odour. TBN is the determination of the alkalinity of the lubricant. The high temperature leads to the formation of alkaline lubricants. The lubricant is changed when the TBN is depleted to 50%. Due to the component's degradation, the ferrous particle concentration increases in the oil.

The ferrous particle presence in the lubricant can also be one of the criteria for condition monitoring. The increase in the concentration of ferrous particles can trigger the progression of the wear in components and depict more metal-to-metal contact—the ferrous particle measured in particles per million (ppm). The ISO and NAS provide the codes for the cleanliness of the lubricant. Spectroscopic studies are carried out to differentiate between virgin oil from recycled oil. The spectrometric study shows different bonds present in the lubricant, which determine the presence of volatile hydrocarbons, solid products (asphalts, carbenes), gases (CO, CO2), liquids (alcohols, acids, eather, resins, ketones, aldehydes etc.), and chemical products. The spectrometric analysis provides information regarding the diagnosis of the component within the error span of 0.5%-1%. The ASTM standard provides information about the relation of wavelength with substantial oil functional groups.

The FTIR spectroscopy is the tool to estimate the presence of the oxide's residue in the oil, the purification of the oil, qualitatively and quantitative elemental[134]. Salt slides are used as the windows; lubricant or oil samples are initially dispersed over the salt window; infrared radiation is through over the window, and the lubricant spectra are acquired. The NaCl and KBr slides are used because the salt has excellent transmittance for the infrared range of the spectrum. The information generated can be used as the diagnosis for the lubricant, and the correspondence can be used to determine the component's health. Table 1 shows the relation of the transmittance/ absorption with the specific functional group. In the presence of the compound, new-formed functional groups in virgin and used oil can be detected. The newly formed compound peaks are seen in the spectra, and the depletion of the bond or compound shows the peak's disappearance.

Table 1 The functional group and associated frequency [147–150]

Group frequency (cm^{-1})	Functional group
3600-3200 and 1600-1200	H-O-H stretching
2200-1800 and 2000-1650	O=C=O stretching and C-H bending
3500-3300 and 1700-1500	N-H stretching (amine) and N-H bending (amine)
3800-3500 and 1400-1300	O-H bending (phenol)
1200-800, 3000-2800 and 500-400	ZnO
1700-1600 and 1000-650	C=C stretching (alkane, ketone)
1600-1300	N-O stretch and C-H stretch (alkane, aldehyde)
900-700	C-H bending
1400-1000	O-H bending, S=O stretching, C-N stretching, C-O stretching (Carboxylic acid, sulfate, aromatic amine, ester)

Conclusions

Complete diagnosis techniques based on the lubrication and wear debris are discussed above. The oil and wear techniques provide the closest information on the concerned component. These techniques are not working for the faults like cracks etc. The following suggestions about research prospects can be drawn from the above study:

a. The gearbox should be considered a single unit is combining bearing, shaft, seals and gears. The fault in one can act as a catalyst for the failure in the other element. So, the global faults deserve some investigation.
b. Mild wear is a progressive type of wear and supplements the other processes like fatigue failure and bending failure. So, the optimal limit of mild wear should be defined to avoid the other failure mechanism.
c. The distinguishing source of wear debris deserves some investigation.

Nomenclature

$g_o(x,t)$ Unloaded geometric gap $\left[\frac{x^2}{2R_{eq}(t)}\right]$
R_{eq} The equivalent radius of curvature $\left[\frac{1}{R_1(t)}+\frac{1}{R_2(t)}\right]^{-1}$
$S_1(x,t)$ and $S_2(x,t)$ Surface roughness profiles in rolling and sliding direction
μ_f Friction coefficient
IPCA Index of particle coverage area
c Total coverage area of wear debris
w_a Length of ferrographic plate
w_b Width of ferrographic plate
D_L Particles greater than 5 microns
D_S Particles less than 5 microns
$'\alpha' and '\beta'$ Weibull parameter
$'\delta_S' and '\delta_T'$ Fractal descriptor
R_q Standard deviation/roughness of the surface
R_{sk} Skewness
R_{ku} Kurtosis
ξ Damping ratio and pressure viscosity coefficient
E' Dimensionless elasticity modulus
u Effective peripheral velocity
η_o Absolute viscosity (cP)
h_{min} Minimum oil film thickness
Δ Specific film parameter
μ Lubricant dynamic viscosity
$\bar{\mu}$ Non-dimensional lubricant viscosity
τ_o Lubricant reference stress
τ_m Viscous shear stress $\tau_m = \tau_o \sinh^{-1}\left[\frac{\mu u_s(t)}{(\tau_o \mathrm{h})}\right]$
$u_s(t)$ Time-dependent sliding velocity
$u_r(t)$ Time-dependent sliding velocity in x-direction
$v_r(t)$ Time-dependent sliding velocity in y-direction
h Film thickness
p Pressure
$\bar{p}$ Dimensionless pressure
ρ Lubricant density
ρ_o Lubricant density at ambient pressure

References

[1] Höhn, B. R., Michaelis, K., and Otto, H. P., 2009, "Minimised Gear Lubrication by a Minimum Oil/Air Flow Rate," Wear, 266(3–4), pp. 461–467.
[2] Kolekar, A. S., Olver, A. V., Sworski, A. E., and Lockwood, F. E., 2014, "Windage and Churning Effects in Dipped Lubrication," J. Tribol., 136(2), p. 021801.
[3] Taylor, P., 2010, "An Experimental Investigation of the Influence of the Lubricant Viscosity and Additives on Gear Wear An Experimental Investigation of the Influence of the Lubricant Viscosity and Additives on Gear Wear," (934204318).
[4] Sheng, S., 2016, "Monitoring of Wind Turbine Gearbox Condition through Oil and Wear Debris Analysis: A Full-Scale Testing Perspective," Tribol. Trans., 59(1), pp. 149–162.
[5] Sarkar, C., and Hirani, H., 2015, "Synthesis and Characterization of Nano-Particles Based Magnetorheological Fluids for Brake," Tribol. Online, 10(4), pp. 282–294.
[6] Hirani, H., Athre, K., and Biswas, S., 1998, "Rapid and Globally Convergent Method for Dynamically Loaded Journal Bearing Design," Proc. Inst. Mech. Eng. Part J J. Eng. Tribol., 212(3), pp. 207–213.
[7] Hirani, H., 2009, "Root Cause Failure Analysis of Outer Ring Fracture of Four-Row Cylindrical Roller Bearing," Tribol. Trans., 52(2), pp. 180–190.
[8] Lijesh, K. P., Muzakkir, S. M., Hirani, H., and Thakre, G. D., 2016, "Control on Wear of Journal Bearing Operating in Mixed Lubrication Regime Using Grooving Arrangements," Ind. Lubr. Tribol., 68(4), pp. 458–465.
[9] Lijesh, K. P., and Hirani, H., 2015, "Magnetic Bearing Using Rotation Magnetized Direction Configuration," J. Tribol., 137(4), pp. 1–11.
[10] Hirani, H., 2005, "Multiobjective Optimization of Journal Bearing Using Mass Conserving and Genetic Algorithms," Proc. Inst. Mech. Eng. Part J J. Eng. Tribol., 219(3), pp. 235–248.
[11] Goilkar, S. S., and Hirani, H., 2009, "Design and Development of a Test Setup for Online Wear Monitoring of Mechanical Face Seals Using a Torque Sensor," Tribol. Trans., 52(1), pp. 47–58.
[12] Hirani, H., and Goilkar, S. S., 2011, "Rotordynamic Analysis of Carbon Graphite Seals of a Steam Rotary Joint," IUTAM Bookseries, 25, pp. 253–262.
[13] Hirani, H., and Rao, T. V. V. L. N., 2003, "Optimization of Journal Bearing Groove Geometry Using Genetic Algorithm," NaCoMM03, IIT Delhi, India, 1, pp. 1–9.
[14] Ghosh, K., Mazumder, S., Kumar Singh, B., Hirani, H., Roy, P., and Mandal, N., 2020, "Tribological Property Investigation of Self-Lubricating Molybdenum-Based Zirconia Ceramic Composite Operational at Elevated Temperature," J. Tribol., 142(2), pp. 1–8.
[15] Lijesh, K. P., Kumar, D., and Hirani, H., 2017, "Effect of Disc Hardness on MR Brake Performance," Eng. Fail. Anal., 74, pp. 228–238.
[16] Lijesh, K. P., and Hirani, H., 2015, "Modeling and Development of RMD Configuration Magnetic Bearing," Tribol. Ind., 37(2), pp. 225–235.
[17] Goilkar, S. S., and Hirani, H., 2010, "Parametric Study on Balance Ratio of Mechanical Face Seal in Steam Environment," Tribol. Int., 43(5–6), pp. 1180–1185.
[18] Hirani, H., Athre, K., and Biswas, S., 2001, "A Simplified Mass Conserving Algorithm for Journal Bearing under Large Dynamic Loads," Int. J. Rotating Mach., 7(1), pp. 41–51.
[19] Sarkar, C., and Hirani, H., 2015, "Synthesis and Characterisation of Nano Silver Particle-Based Magnetorheological Fluids for Brakes," Def. Sci. J., 65(3), pp. 252–258.
[20] Muzakkir, S. M., Hirani, H., and Thakre, G. D., 2013, "Lubricant for

Heavily Loaded Slow-Speed Journal Bearing," Tribol. Trans., 56(6), pp. 1060–1068.
[21] Hirani, H., and Manjunatha, C. S., 2007, "Performance Evaluation of a Magnetorheological Fluid Variable Valve," Proc. Inst. Mech. Eng. Part D J. Automob. Eng., 221(1), pp. 83–93.
[22] Lijesh, K. P., Muzakkir, S. M., and Hirani, H., 2015, "Experimental Tribological Performance Evaluation of Nano Lubricant Using Multi-Walled Carbon Nano-Tubes (MWCNT)," Int. J. Appl. Eng. Res., 10(6), pp. 14543–14550.
[23] Ghosh, K., Mazumder, S., Hirani, H., Roy, P., and Mandal, N., 2021, "Enhancement of Dry Sliding Tribological Characteristics of Perforated Zirconia Toughened Alumina Ceramic Composite Filled with Nano MoS2 in High Vacuum," J. Tribol., 143(6), pp. 1–9.
[24] Ebner, M., Yilmaz, M., Lohner, T., Michaelis, K., Höhn, B. R., and Stahl, K., 2018, "On the Effect of Starved Lubrication on Elastohydrodynamic (EHL) Line Contacts," Tribol. Int., 118(June), pp. 515–523.
[25] Fitch, J., and Corporation, N., 2016, "The Benefits of Utilizing Wear Debris Analysis in Industrial Machinery," pp. 1–8.
[26] Manton, S. M., and Donoghue, J. P. O., "Gear Lubricant Testing Machines- Are They Useful," pp. 1–4.
[27] Burla, R. K., Seshu, P., Hirani, H., Sajanpawar, P. R., and Suresh, H. S., 2003, "Three Dimensional Finite Element Analysis of Crankshaft Torsional Vibrations Using Parametric Modeling Techniques," SAE Tech. Pap., 112, pp. 2330–2337.
[28] Hirani, H., Athre, K., and Biswas, S., 2000, "Comprehensive Design Methodology for an Engine Journal Bearing," Proc. Inst. Mech. Eng. Part J J. Eng. Tribol., 214(4), pp. 401–412.
[29] Gupta, S., and Hirani, H., 2011, "Optimization of Magnetorheological Brake," Am. Soc. Mech. Eng. Tribol. Div. TRIB, pp. 405–406.
[30] Hirani, H., Athre, K., and Biswas, S., 2001, "Lubricant Shear Thinning Analysis of Engine Journal Bearings," Tribol. Trans., 44(1), pp. 125–131.
[31] Muzakkir, S. M., Lijesh, K. P., and Hirani, H., 2016, "Influence of Surfactants on Tribological Behaviors of MWCNTs (Multi-Walled Carbon Nano-Tubes)," Tribol. - Mater. Surfaces Interfaces, 10(2), pp. 74–81.
[32] Lijesh, K. P., and Hirani, H., 2015, "Design of Eight Pole Radial Active Magnetic Bearing Using Monotonicity," 9th Int. Conf. Ind. Inf. Syst. ICIIS 2014.
[33] Lijesh, K. P., and Hirani, H., 2015, "Design and Development of Halbach Electromagnet for Active Magnetic Bearing," Prog. Electromagn. Res. C, 56(January), pp. 173–181.
[34] Lijesh, K. P., Muzakkir, S. M., and Hirani, H., 2016, "Rheological Measurement of Redispersibility and Settling to Analyze the Effect of Surfactants on MR Particles," Tribol. - Mater. Surfaces Interfaces, 10(1), pp. 53–62.
[35] Sukhwani, V. K., and Hirani, H., 2007, "Synthesis and Characterization of Low Cost Magnetorheological (MR) Fluids," Behav. Mech. Multifunct. Compos. Mater. 2007, 6526, p. 65262R.
[36] Samanta, P., and Hirani, H., 2008, "An Overview of Passive Magnetic Bearings," Proc. STLE/ASME Int. Jt. Tribol. Conf., pp. 1–3.
[37] Lijesh, K. P., and Hirani, H., 2016, "Failure Mode and Effect Analysis of Active Magnetic Bearings," Tribol. Ind., 38(1), pp. 90–101.
[38] Goilkar, S. S., and Hirani, H., 2009, "Tribological Characterization of Carbon Graphite Secondary Seal," Indian J. Tribol., 4(2), pp. 1–6.
[39] Samanta, P., and Hirani, H., 2007, "A Simplified Optimization Approach for Permanent Magnetic Journal Bearing," Indian J. Tribol., 2(2), pp. 23–28.
[40] Samanta, P., Hirani, H., Mitra, A., Kulkarni, A. M., and Fernandes, B. G., 2005, "Test Setup for Magneto Hydrodynamic Journal Bearing," NaCoMM, pp. 298–303.
[41] Athre, K., and Biswas, S., 2000, "A Hybrid Solution Scheme for Performance Evaluation of Crankshaft Bearings," J. Tribol., 122(4), pp. 733–740.
[42] Lijesh, K. P., Kumar, D., and Hirani, H., 2017, "Synthesis and Field Dependent Shear Stress Evaluation of Stable MR Fluid for Brake Application," Ind. Lubr. Tribol., 69(5), pp. 655–665.
[43] Sarkar, C., and Hirani, H., 2017, "Experimental Studies on Magnetorheological Brake Containing Plane, Holed and Slotted Discs," Ind. Lubr. Tribol., 69(2), pp. 116–122.
[44] Hirani, H., Athre, K., and Biswas, S., 1999, "Dynamic Analysis of Engine Bearings," Int. J. Rotating Mach., 5(4), pp. 283–293.
[45] Lijesh, K. P., Muzakkir, S. M., and Hirani, H., 2016, "Failure Mode and Effect Analysis of Passive Magnetic Bearing," Eng. Fail. Anal., 62, pp. 1–20.
[46] Lijesh, K. P., Kumar, D., Muzakkir, S. M., and Hirani, H., 2018, "Thermal and Frictional Performance Evaluation of Nano Lubricant with Multi Wall Carbon Nano Tubes (MWCNTs) as Nano-Additive," AIP Conf. Proc., 1953(May), pp. 1–6.
[47] Lijesh, K. P., and Hirani, H., 2017, "Design and Development of Permanent Magneto-Hydrodynamic Hybrid Journal Bearing," J. Tribol., 139(4), pp. 1–9.
[48] "Polymer Composites - 2021 - Antil - An Improvement in Drilling of SiCp Glass Fiber-reinforced Polymer Matrix Composites.Pdf."
[49] Antil, P., Singh, S., and Singh, P. J., 2018, "Taguchi's Methodology Based Electrochemical Discharge Machining of Polymer Matrix Composites," Procedia Manuf., 26, pp. 469–473.
[50] Antil, P., Singh, S., and Manna, A., 2020, "Experimental Investigation During Electrochemical Discharge Machining (ECDM) of Hybrid Polymer Matrix Composites," Iran. J. Sci. Technol. - Trans. Mech. Eng., 44(3), pp. 813–824.
[51] Antil, P., Kumar Antil, S., Prakash, C., Królczyk, G., and Pruncu, C., 2020, "Multi-Objective Optimization of Drilling Parameters for Orthopaedic Implants," Meas. Control (United Kingdom), 53(9–10), pp. 1902–1910.
[52] Antil, P., Singh, S., Kumar, S., Manna, A., and Katal, N., 2019, "Taguchi and Multi-Objective Genetic Algorithm-Based Optimization during Ecdm of Sicp /Glass Fibers Reinforced Pmcs," Indian J. Eng. Mater. Sci., 26(3–4), pp. 211–219.
[53] Antil, P., Singh, S., and Manna, A., 2018, "SiCp/Glass Fibers Reinforced Epoxy Composites: Wear and Erosion Behavior," Indian J. Eng. Mater. Sci., 25(2), pp. 122–130.
[54] Antil, P., Singh, S., and Manna, A., 2019, "Analysis on Effect of Electroless Coated SiCp on Mechanical Properties of Polymer Matrix Composites," Part. Sci. Technol., 37(7), pp. 787–794.
[55] Antil, P., Singh, S., and Manna, A., 2018, "Genetic Algorithm Based Optimization of ECDM Process for Polymer Matrix Composite," Mater. Sci. Forum, 928 MSF, pp. 144–149.
[56] Antil, P., 2020, "Modelling and Multi-Objective Optimization during ECDM of Silicon Carbide Reinforced Epoxy Composites," Silicon, 12(2), pp. 275–288.
[57] Kharb, S. S., Antil, P., Singh, S., Antil, S. K., Sihag, P., and Kumar, A., 2021, "Machine Learning-Based Erosion Behavior of Silicon Carbide Reinforced Polymer Composites," Silicon, 13(4), pp. 1113–1119.
[58] Antil, P., 2019, "Experimental Analysis on Wear Behavior of PMCs Reinforced with Electroless Coated Silicon Carbide Particulates," Silicon, 11(4), pp. 1791–1800.
[59] Antil, P., Singh, S., and Manna, A., 2018, "Glass Fibers/SiCp Reinforced Epoxy Composites: Effect of Environmental Conditions," J. Compos. Mater., 52(9), pp. 1253–1264.
[60] Antil, P., Singh, S., Singh, S., Prakash, C., and Pruncu, C. I., 2019, "Metaheuristic Approach in Machinability Evaluation of Silicon Carbide Particle/Glass Fiber–Reinforced Polymer Matrix Composites during Electrochemical Discharge Machining Process," Meas. Control (United Kingdom), 52(7–8), pp. 1167–1176.
[61] Antil, S. K., Antil, P., Singh, S., Kumar, A., and Pruncu, C. I., 2020, "Artificial Neural Network and Response Surface Methodology Based Analysis on Solid Particle Erosion Behavior of Polymer Matrix Composites," Materials (Basel)., 13(6).
[62] Antil, P., Singh, S., Kumar, S., Manna, A., and Pruncu, C. I., 2019, "Erosion Analysis of Fiber Reinforced Epoxy Composites," Mater. Res. Express, 6(10), p. 106520.
[63] Amarnath, M., and Sujatha, C., 2015, "Surface Contact Fatigue Failure Assessment in Spur Gears Using Lubricant Film Thickness and Vibration Signal Analysis," Tribol. Trans., 58(2), pp. 327–336.
[64] Sukhwani, V. K., Lakshmi, V., & Hirani, H., 2006, "Performance Evaluation of MR Brake: An Experimental Study," Indian J. Tribol., 1, pp. 47–52.
[65] Talluri, S. K., & Hirani, H., 2003, "Parameter Optimization Of Journal Bearing Using Genetic Algorithm," Indian J. Tribol., 2(1–2), pp. 7–21.

[66] Sukhwani, V. K., Hirani, H., & Singh, T., 2007, "Synthesis and Performance Evaluation of Magnetorheological (MR) Grease," 74th NLGI Annu. Meet. Scottsdale, Arizona, USA.
[67] Sukhwani, V. K., Hirani, H., & Singh, T., 2007, "Synthesis of Magnetorheological Grease," Greasetech India.
[68] Sukhwani, V. K., Hirani, H., & Singh, T., 2008, "Synthesis and Performance Evaluation of Magnetorheological (MR) Grease.," NLGI, Natl. Lubr. Grease Inst., 71(10), pp. 10–21.
[69] Hirani, H., & Dani, S., 2005, "Variable Valve Actuation Mechanism Using Magnetorheological Fluid," World Tribol. Congr., 42029, pp. 569–570.
[70] Shankar, M., Sandeep, S., & Hirani, H., 2006, "Active Magnetic Bearing," Indian J. Tribol., 1, pp. 15–25.
[71] Hirani, H., 2014, "Wear Mechanisms."
[72] Hirani, H., Athre, K., & Biswas, S., 2000, "Transient Trajectory of Journal in Hydodynamic Bearing," Appl. Mech. Eng., 5(2), pp. 405–418.
[73] Sukhwani, V. K., Hirani, H., & Singh, T., 2009, "Performance Evaluation of a Magnetorheological Grease Brake," Greasetech India, 9(4), pp. 5–11.
[74] Hirani, H., 2016, *Fundamental of Engineering Tribology with Applications*.
[75] Amarnath, M., and Lee, S. K., 2015, "Assessment of Surface Contact Fatigue Failure in a Spur Geared System Based on the Tribological and Vibration Parameter Analysis," Meas. J. Int. Meas. Confed., 76, pp. 32–44.
[76] Wang, S., Wu, T., Wu, H., and Kwok, N., 2017, "Modeling Wear State Evolution Using Real-Time Wear Debris Features," Tribol. Trans., 60(6), pp. 1022–1032.
[77] Cummins, R. A., Doyle, E. D., and Rebecchi, B., 1974, "Wear Damage to Spur Gears," Wear, 27(1), pp. 115–120.
[78] Dharmender, Darpe, A. K., and Hirani, H., 2020, *Classification of Stages of Wear in Spur Gears Based on Wear Debris Morphology*.
[79] Kumar, A., Antil, S. K., Rani, V., Antil, P., and Jangra, D., 2020, "Characterization on Physical , Mechanical , and Morphological Properties of Indian Wheat Crop," pp. 1–18.
[80] Kumar, P., Hirani, H., and Kumar Agrawal, A., 2019, "Effect of Gear Misalignment on Contact Area: Theoretical and Experimental Studies," Meas. J. Int. Meas. Confed., 132, pp. 359–368.
[81] Kumar, P., Hirani, H., and Agrawal, A. K., 2019, "Modeling and Simulation of Mild Wear of Spur Gear Considering Radial Misalignment," Iran. J. Sci. Technol. - Trans. Mech. Eng., 43(s1), pp. 107–116.
[82] Kumar, P., Hirani, H., and Agrawal, A., 2017, "Fatigue Failure Prediction in Spur Gear Pair Using AGMA Approach," Mater. Today Proc., 4(2), pp. 2470–2477.
[83] Kumar, P., Hirani, H., and Agrawal, A. K., 2018, "Online Condition Monitoring of Misaligned Meshing Gears Using Wear Debris and Oil Quality Sensors," Ind. Lubr. Tribol., 70(4), pp. 645–655.
[84] Kumar, P., Hirani, H., and Agrawal, A., 2015, "Scuffing Behaviour of EN31 Steel under Dry Sliding Condition Using Pin-on-Disc Machine," Mater. Today Proc., 2(4–5), pp. 3446–3452.
[85] Shah, H., and Hirani, H., 2014, "Online Condition Monitoring of Spur Gears," Int. J. Cond. Monit., 4(1), pp. 15–22.
[86] Hirani, H., 2009, "Online Wear Monitoring of Spur Gears," Indian J. Tribol., 4(2), pp. 38–43.
[87] Hirani, H., 2012, "Online Condition Monitoring of High Speed Gears Using Vibration and Oil Analyses," Therm. fluid Manuf. Sci. Narosa Publ. House, pp. 21–28.
[88] Scott, D., 1975, "Debris Examination — a Prognostic Approach to Failure Prevention," Wear, 34(1), pp. 15–22.
[89] Kumar, P., Hirani, H., and Agrawal, A. K., 2018, "Online Condition Monitoring of Misaligned Meshing Gears Using Wear Debris and Oil Quality Sensors," Ind. Lubr. Tribol., 70(4), pp. 645–655.
[90] Loutas, T. H., Roulias, D., Pauly, E., and Kostopoulos, V., 2011, "The Combined Use of Vibration, Acoustic Emission and Oil Debris on-Line Monitoring towards a More Effective Condition Monitoring of Rotating Machinery," Mech. Syst. Signal Process., 25(4), pp. 1339–1352.
[91] Feng, S., Fan, B., Mao, J., and Xie, Y., 2015, "Prediction on Wear of a Spur Gearbox by On-Line Wear Debris Concentration Monitoring," Wear, 336–337, pp. 1–8.
[92] Mimoza Naseska, and ˇZitnik, M., 2016, "Fourier Transform Infrared Spectroscopy," pp. 1–12.
[93] Davis, J. R., 2005, *Gear Materials, Properties, and Manufacture*, ASM International.
[94] Andersson, S., 1977, "Initial Wear of Gears," Tribol. Int., 10(4), pp. 206–210.
[95] Iwai, Y., Honda, T., Miyajima, T., Yoshinaga, S., Higashi, M., and Fuwa, Y., 2010, "Quantitative Estimation of Wear Amounts by Real Time Measurement of Wear Debris in Lubricating Oil," Tribol. Int., 43(1–2), pp. 388–394.
[96] Wear, M., Evolution, S., Real, U., Wear, T., Features, D., Wang, S., Wu, T., Wu, H., and Kwok, N., "Modelling Wear State Evolution Using Real Time Wear Debris Features," pp. 1–44.
[97] Khan, M. A., and Starr, A. G., 2006, "Wear Debris: Basic Features and Machine Health Diagnostics," Insight Non-Destructive Test. Cond. Monit., 48(8), pp. 470–476.
[98] Stachowiak, G. P., Stachowiak, G. W., and Podsiadlo, P., 2008, "Automated Classification of Wear Particles Based on Their Surface Texture and Shape Features," Tribol. Int., 41(1), pp. 34–43.
[99] Podsiadlo, P., and Stachowiak, G. W., 1998, "Evaluation of Boundary Fractal Methods for the Characterization of Wear Particles," Wear, 217(1), pp. 24–34.
[100] Myshkin, N. K., Kwon, O. K., Grigoriev, A. Y., Ahn, H. S., and Kong, H., 1997, "Classification of Wear Debris Using a Neural Network," Wear, 203–204(96), pp. 658–662.
[101] Peng, Z., and Kessissoglou, N., 2003, "An Integrated Approach to Fault Diagnosis of Machinery Using Wear Debris and Vibration Analysis," Wear, 255(7–12), pp. 1221–1232.
[102] Dempsey, P. J., Lewicki, D. G., and Decker, H. J., 2004, "Investigation of Gear and Bearing Fatigue Damage Using Debris Particle Distributions," Nasa / Tm - 2004-212883 Arl-Tr-3133, 298(0704), p. 16.
[103] Podsiadlo, P., and Stachowiak, G. W., 1998, "The Development of the Modified Hurst Orientation Transform for the Characterization of Surface Topography of Wear Particles," Tribol. Lett., 4, pp. 215–229.
[104] S L, M., Geometry, R., and Analysis, G., "Knowledge Based Wear Particle Analysis."
[105] Myshkin, N. K., Kong, H., Grigoriev, A. Y., and Yoon, E. S., 2001, "The Use of Color in Wear Debris Analysis," Wear, 250(251), pp. 1218–1226.
[106] Fitch, B., 2018, "Anatomy of Wear Debris," Mach. Lubr., pp. 1–7.
[107] Tan, C. K., Irving, P., and Mba, D., 2007, "A Comparative Experimental Study on the Diagnostic and Prognostic Capabilities of Acoustics Emission, Vibration and Spectrometric Oil Analysis for Spur Gears," Mech. Syst. Signal Process., 21(1), pp. 208–233.
[108] Hamilton, A., and Quail, F., 2011, "Detailed State of the Art Review for the Different Online/Inline Oil Analysis Techniques in Context of Wind Turbine Gearboxes," J. Tribol., 133(4), p. 044001.
[109] Vähäoja, P., Välimäki, I., Roppola, K., Kuokkanen, T., and Lahdelma, S., 2008, "Wear Metal Analysis of Oils," Crit. Rev. Anal. Chem., 38(2), pp. 67–83.
[110] Henneberg, M., Jørgensen, B., and Eriksen, R. L., 2016, "Oil Condition Monitoring of Gears Onboard Ships Using a Regression Approach for Multivariate T2 Control Charts," J. Process Control, 46, pp. 1–10.
[111] Fan, B., Li, B., Feng, S., Mao, J., and Xie, Y. B., 2017, "Modeling and Experimental Investigations on the Relationship between Wear Debris Concentration and Wear Rate in Lubrication Systems," Tribol. Int., 109(28), pp. 114–123.
[112] Watson, H., 1969, "Designing Against Wear - Wear of Gears," Tribology, pp. 212–216.
[113] Ognjanovic, M., 2004, "Progressive Gear Teeth Wear and Failure Probability Modeling," Tribol. Ind., 26(3–4), pp. 44–49.
[114] Muniyappa, A., Chandramohan, S., and Seethapathy, S., 2010, "Detection and Diagnosis of Gear Tooth Wear through Metallurgical and Oil Analysis," Tribol. Online, 5(2), pp. 102–110.
[115] Randall, R. B., 2011, *Vibration-Based Condition Monitoring*, John Wiley & Sons Ltd.
[116] Sondhiya, O., and Gupta, A., 2012, "Wear Debris Analysis of Automotive Engine Lubricating Oil Using By Ferrography," Ijeit.Com, 2(5), pp. 46–54.
[117] Wu, J., Mao, J., Cao, W., and Xie, Y. B., 2014, "Characterization of Wear-Debris Group in on-Line Visual Ferrographic Images,"

Proc. Inst. Mech. Eng. Part J J. Eng. Tribol., 228(11), pp. 1298–1307.
[118] Yan, L., Youbai, X., Fang, Z., and Zhigang, Y., 1998, "Revision to the Concept of Equilibrium Concentration of Particles in Lubrication System of Machines," Wear, 215(1–2), pp. 205–210.
[119] Sarkar, A. D., 1983, "The Role of Wear Debris in the Study of Wear," Wear, 90(1), pp. 39–47.
[120] Roylance, B. J., 2000, "Wear Debris and Associated Wear Phenomena-Fundamental Research and Practice," Proc. Inst. Mech. Eng. Part J J. Eng. Tribol., 214(1), pp. 79–105.
[121] Raadnui, S., 2005, "Wear Particle Analysis - Utilization of Quantitative Computer Image Analysis: A Review," Tribol. Int., 38(10), pp. 871–878.
[122] Yuan, W., Chin, K. S., Hua, M., Dong, G., and Wang, C., 2016, "Shape Classification of Wear Particles by Image Boundary Analysis Using Machine Learning Algorithms," Mech. Syst. Signal Process., 72–73, pp. 346–358.
[123] Cho, U., and Tichy, J. A., 2000, "Quantitative Correlation of Wear Debris Morphology: Grouping and Classification," Tribol. Int., 33(7), pp. 461–467.
[124] Laghari, M. S., 2003, "Recognition of Texture Types of Wear Particles," Neural Comput. Appl., 12(1), pp. 18–25.
[125] Myshkin, N. K., and Grigoriev, A. Y., 2008, "Morphology: Texture, Shape, and Color of Friction Surfaces and Wear Debris in Tribodiagnostics Problems," J. Frict. Wear, 29(3), pp. 192–199.
[126] Roylance, B. J., and Raadnui, S., 1994, "The Morphological Attributes of Wear Particles - Their Role in Identifying Wear Mechanisms," Wear, 175(1–2), pp. 115–121.
[127] Liu, H., Mao, K., Zhu, C., and Xu, X., 2012, "Mixed Lubricated Line Contact Analysis for Spur Gears Using a Deterministic Model," J. Tribol., 134(2), p. 021501.
[128] Akbarzadeh, S., and Khonsari, M. M., 2009, "Prediction of Steady State Adhesive Wear in Spur Gears Using the EHL Load Sharing Concept," J. Tribol., 131(2), p. 024503.
[129] Townsend, D. P., Zaretsky, E. V., and Scibbe, H. W., 1989, "Lubricant and Additive Effects on Spur Gear Fatigue Life," J. Synth. Lubr., 6(2), pp. 83–106.
[130] Masjedi, M., and Khonsari, M. M., 2015, "On the Prediction of Steady-State Wear Rate in Spur Gears," Wear, 342–343, pp. 234–243.
[131] Townsend, D. P., and Shimski, J., 1994, "Evaluation of the EHL Film Thickness and Extreme Pressure Additives on Gear Surface Fatigue Life," NASA Tech. Memo., pp. 0–9.
[132] Townsend, D. P., and Zaretsky, E. V, 1985, "Effect of Five Lubricants on Life of AISI 9310 Spur Gears," NASA STI/Recon Tech. Rep. N, 85(June 1991), p. 16099.
[133] Amarnath, M., Sujatha, C., and Swarnamani, S., 2009, "Experimental Studies on the Effects of Reduction in Gear Tooth Stiffness and Lubricant Film Thickness in a Spur Geared System," Tribol. Int., 42(2), pp. 340–352.
[134] Amarnath, M., and Lee, S. K., 2015, "Assessment of Surface Contact Fatigue Failure in a Spur Geared System Based on the Tribological and Vibration Parameter Analysis," Measurement, 76, pp. 32–44.
[135] Krantz, T. L., 2015, "On the Correlation of Specific Film Thickness and Gear Pitting Life," Gear Technol., (February), pp. 52–62.
[136] Brandão, J. A., Cerqueira, P., Seabra, J. H. O., and Castro, M. J. D., 2016, "Measurement of Mean Wear Coefficient during Gear Tests under Various Operating Conditions," Tribol. Int., 102, pp. 61–69.
[137] Peng, Z., and Kirk, T. B., 1999, "Wear Particle Classification in a Fuzzy Grey System," Wear, 225–229(PART II), pp. 1238–1247.
[138] Bartz, W. J., and Krijger, V., 1973, "Pitting Fatigue of Gears - Some Ideas on a p p e a r a n c e , m e c h a n i s m and Lubricant Influence," (October), pp. 191–195.
[139] Stachowiak, G. W., 2000, "Particle Angularity and Its Relationship to Abrasive and Erosive Wear," Wear, 241(2), pp. 214–219.
[140] Peng, Z., 2002, "An Integrated Intelligence System for Wear Debris Analysis," Wear, 252(9–10), pp. 730–743.
[141] Peng, Z., and Kirk, T. B., 1998, "Computer Image Analysis of Wear Particles in Three-Dimensions for Machine Condition Monitoring," Wear, 223(1–2), pp. 157–166.
[142] Kirk, T. B., Panzera, D., Anamalay, R. V., and Xu, Z. L., 1995, "Computer Image Analysis of Wear Debris for Machine Condition Monitoring and Fault Diagnosis," Wear, 181–183(PART 2), pp. 717–722.
[143] Podsiadlo, P., and Stachowiak, G. W., 2000, "Scale-Invariant Analysis of Wear Particle Surface Morphology I: Theoretical Background, Computer Implementation and Technique Testing," Wear, 242(1–2), pp. 160–179.
[144] Podsiadlo, P., and Stachowiak, G. W., 2000, "Scale-Invariant Analysis of Wear Particle Surface Morphology II. Fractal Dimension," Wear, 242(1–2), pp. 180–188.
[145] Stachowiak, G. W., 1998, "Numerical Characterization of Wear Particles Morphology and Angularity of Particles and Surfaces," Tribol. Int., 31(1–3), pp. 139–157.
[146] Tian, Y., Wang, J., Peng, Z., and Jiang, X., 2012, "A New Approach to Numerical Characterisation of Wear Particle Surfaces in Three-Dimensions for Wear Study," Wear, 282–283, pp. 59–68.
[147] "IR-Frequencies" [Online]. Available: http:// www2.ups.edu/ faculty/ hanson/ Spectroscopy/ IR/IRfrequencies.html. [Accessed: 17-Oct-2019].
[148] Al-Ghouti, M. A., and Al-Atoum, L., 2009, "Virgin and Recycled Engine Oil Differentiation: A Spectroscopic Study," J. Environ. Manage., 90(1), pp. 187–195.
[149] "12.8: Infrared Spectra of Some Common Functional Groups - Chemistry LibreTexts" [Online]. Available: https://chem.libretexts.org/Bookshelves/Organic_Chemistry/Map%3A_Organic_Chemistry_(McMurry)/Chapter_12%3A_Structure_Determination%3A_Mass_Spectrometry_and_Infrared_Spectroscopy/12.08_Infrared_Spectra_of_Some_Common_Functional_Groups. [Accessed: 17-Oct-2019].
[150] "Basic Organic Functional Group_reference Chart."